INFLUENCE OF DIFFERENT SURFACE EFFECTS ON THE NUCLEATION OF MICROCRACKS

M. Sauzay[1,2], P. Gilormini[1] and P. Coorevits[3]

[1] Laboratoire de mécanique et technologie,
ENS Cachan/CNRS UMR 8535/Université Paris VI,
61, avenue du Prksident Wilson, 94235 Cachan, France
[2] Ledepp, USINOR Recherche et Développement, 57191 Florange, France
[3] INSSET, 48 rue Raspail, 02100 Saint-Quentin, France

ABSTRACT

High-cycle fatigue of metals involves microplasticity: under low cycling remote stresses, plastic slip occurs in a few grains at the surface of the specimen. It may localize to form persistent slip bands (PSBs) in the well-oriented grains, and cracks eventually nucleate. Our goal is to compare plasticity and crack nucleation for PSBs at the free surface and in the bulk. Cyclic plastic slips in volume PSBs can be evaluated analytically using Eshelby's localization solution for a PSB embedded in an infinite elastic matrix. Plastic slips in surface PSBs have to be estimated using finite element computations. In practical applications, the surface plastic slips are obtained by first computing analytically the result in a bulk PSB, and then multiplying by the corresponding factor, which is independent on the aspect ratio of the PSB. The surface plastic slips are about twice the bulk ones in our model. An application to crack nucleation along PSBs is described, using an energy criteria. The influence of different surface effects like enhanced mesoplasticity or environmental effects can be dicussed in comparison with classical experiments of fatigue using repeated surface removal.

Keywords – free surface, crystallographic glide, persistent slip band, fatigue

INTRODUCTION

High-cycle fatigue of metals involves microplasticity: under low cycling remote stresses, plastic slip occurs, and may localize, in a few grains at the surface of the specimen, and cracks eventually nucleate. This takes place in well-oriented grains (while the others remain almost elastic), such that the largest resolved shear stress applied on their slip systems equals both the maximum applied shear stress (for elastically isotropic grains) and a critical value for the onset of slip. Strain localization mostly occurs within the well-oriented grains where persistent slip bands (PSBs) develop. This is common in face-centered cubic (FCC) metals and in body-centered cubic (BCC) metals in the high temperature mode [1,2]. For a given applied stress level and crystallographic orientation, plastic slip may be larger PSBs at the free surface than in the bulk, and this is likely to induce surface transgranular (Figure 1 PSBs at the free surface of a 316L stainless steel polycrystal **[3]** and Figure 2 PSBs and microcracks at the free surface of a steel polycrystal [4]) [1,2] or intergranular micro-cracks [1,2].

The present paper proposes continuum mechanics analyses to evaluate to which extent the meso-plastic slips in PSBs are enhanced by the free surface, in order to help understanding crack nucleation. The mesoscopic scale is defined by a length of the order of the PSB width (1μm). Stabilization of the plastic behavior is supposed at the mesoscopic scale, following classical observations. Uniaxial remote loading and type B PSBs are considered (Figures 3a and 3b) because they seem to be more damageable than type **A** PSBs. The uniform mesoplastic slips in well-oriented grains (without PSBs in BCC metals in the low temperature mode) have already been computed analytically or numerically in the bulk and at the free surface and are given in [5].

In the present study, following a model of Mura and co-workers [6], an energy criterion is applied to crack nucleation at the free surface and in the bulk considering the microplastic slip irreversihilities. Free surface and environmental effects are partially taken into account. Comparisons with esperimental observations taken from the literature are discussed.

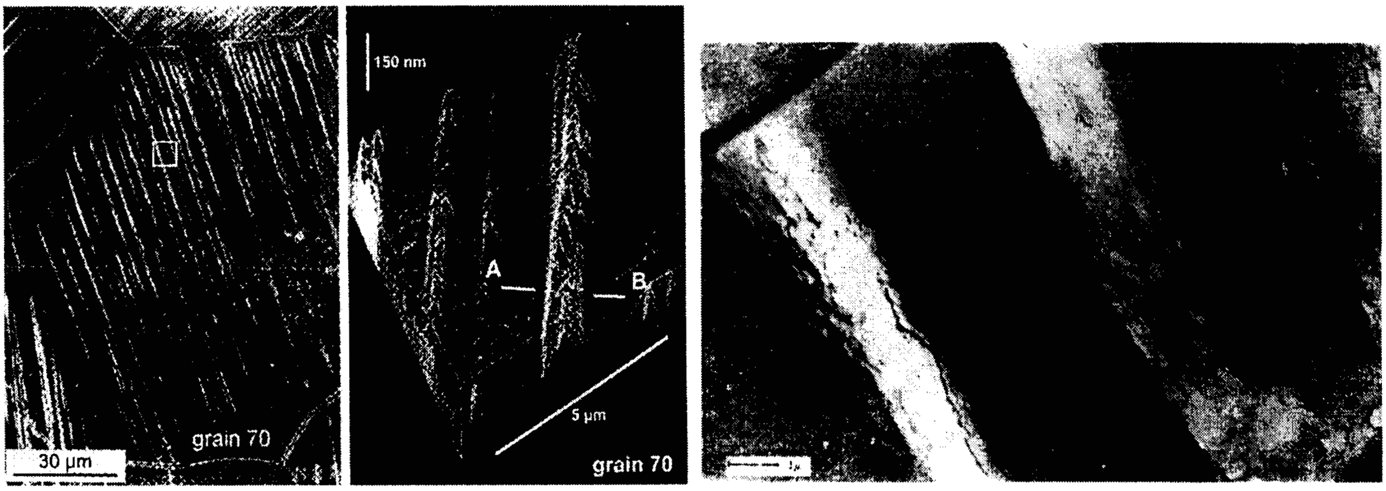

Figure 1: PSBs (SEM and AFM) **[3]**

Figure 2: PSBs and induced microcracks (SEM) [4].

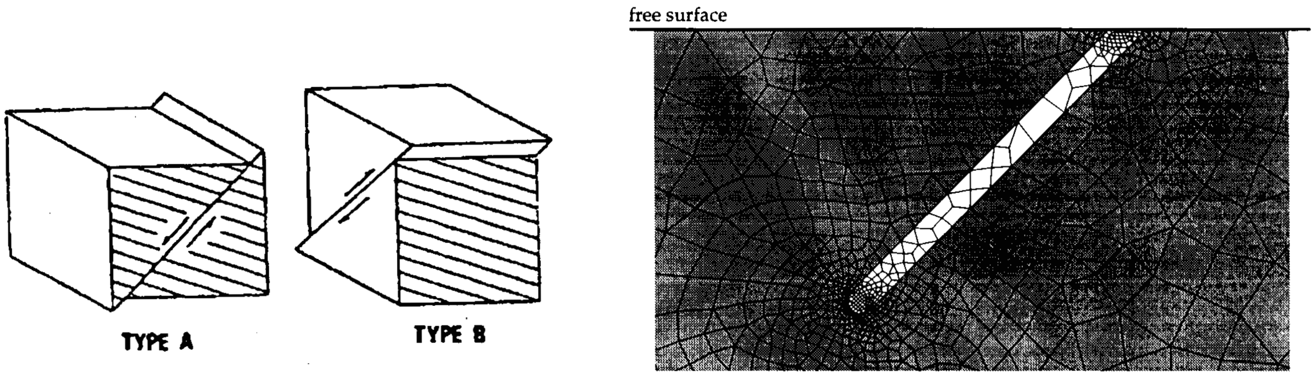

(a) (b)

Figure 3 (a): Type A and B facets [11]. (b): Finite element mesh of a surface PSB of type B (enlarged view of 12% of the total mesh).

MODELISATION

The thickness h of a PSB, parallel to the slip normal $\boldsymbol{n}$, is about 1 pm and the two other dimensions (its length L, parallel to the slip direction $\boldsymbol{m}$, and its width) are about the grain size [7]. For the sake of simplicity, a single PSB in a surface or volume grain is considered and will be the only plastic region in the polycristal, and the elastic anisotropy of the grains will be neglected. The latter assumption implies that the PSB is surrounded by an isotropic elastic medium, and consequently the PSB orientation is governed by the largest remote applied shear stress. Moreover, it will be assumed that the width of the PSB (i.e. its largest dimension seen on the free surface, for surface PSBs) is large enough to be considered infinite in the analyses below in order to use an hypothesis of Plane Deformation (2D FE computations).

In high-cycle fatigue, a small remote uniaxial stress C is applied and single slip is of special concern. Therefore, in a PSB, $\boldsymbol{\varepsilon}^{\mathrm{p}}$ can be written as $\frac{1}{2}\gamma^{\mathrm{p}}(\boldsymbol{n} \otimes \boldsymbol{m} + \boldsymbol{m} \otimes \boldsymbol{n})$, where γ^{p} denotes the slip magnitude in the PSB. The Schmid criterion is used:

$$|\tau| = \tau_c \tag{1}$$

where $\tau = \boldsymbol{m} \cdot \boldsymbol{\sigma} \cdot \boldsymbol{n}$ is the resolved shear stress on the slip system in the PSB. Like for PSBs in a single crystal, isotropic hardening takes place with a saturating shear stress τ_∞:

$$\tau_c = \tau_\infty \left[1 - \left(1 - \frac{\tau_0}{\tau_\infty}\right) \exp\left(-b \int_0^t |\dot{\gamma}^{\mathrm{p}}| \mathrm{d}t\right)\right] \tag{2}$$

where τ_0 denotes the initial critical resolved shear stress, b is a material parameter and $\int_0^t |\dot{\gamma}^{\mathrm{p}}| \mathrm{d}t$ is the cumulated plastic slip. The τ_∞ value obtained in single crystals will be used for grains in polycrystals. For instance, an experimental value of $\tau_\infty = 49\,\mathrm{MPa}$ was measured in ferrite single crystals with 30 wt. ppm carbon [2]. After hardening stabilization, Eqn. 2 can be written more simply as:

$$|\tau| = \tau_\infty\,. \tag{3}$$

TYPE B PSBs

Bulk PSBs

The bulk PSB has an elliptic cross section of thickness h and length L and is embedded in an infinite elastic matrix. The aspect ratio of the band section L/h is the only geometrical parameter because of the infinite extension of the matrix. The localization problem has been solved by Eshelby and leads to the following resolved shear stress in the PSB [8,9]:

$$\tau = \frac{\Sigma}{2} - \frac{\mu}{1-\nu} \frac{\frac{h}{L}}{\left(1+\frac{h}{L}\right)^2} \gamma^{\mathrm{p}} \tag{4}$$

for a $\Sigma/2$ remote shear stress parallel to the band and a uniform plastic slip γ^{p} in the PSB. Note that the shear stress τ is uniform. Defining the applied stress cycles by their mean C, and amplitude C,, the remote stress C oscillates between C, $-\Sigma_{\mathbf{a}}$ and C, $+\Sigma_{\mathbf{a}}$. Consequently, using Eqn. **3** and Eqn. 4, γ^{p} cycles between

$$(1-\nu)\frac{L}{h}\left(1+\frac{h}{L}\right)^2 \frac{\frac{\Sigma_{\mathrm{m}}+\Sigma_{\mathrm{a}}}{2} - \tau_\infty}{\mu} \quad \text{and} \quad (1-\nu)\frac{L}{h}\left(1+\frac{h}{L}\right)^2 \frac{\frac{\Sigma_{\mathrm{m}}-\Sigma_{\mathrm{a}}}{2} + \tau_\infty}{\mu}$$

when hardening saturation is reached. Then, The corresponding plastic slip range when saturation is reached is:

$$\Delta\gamma^{\mathrm{p}} = (1-\nu)\frac{L}{h}\left(1+\frac{h}{L}\right)^2 \frac{C, - 2\tau_\infty}{P} \tag{5}$$

which is uniform in the bulk PSB.

***Surface** PSBs*

Type B surface PSBs require finite element analyses and the solutions are no more uniform. The closed-form expression (5) will be used below for comparisons with the values obtained numerically in surface PSBs, since it is a good approximation of the average given by the finite element method for a volume PSB in an infinite matrix with a mesh similar to Figure 3a (extended, of course, but with a band cross section still poorly close to an ellipse). If generalized plane strain along the PSB width is assumed in the finite element analysis, because of the PSB shape, the problem is two-dimensional and very fine meshes are permitted, which allows varying the PSB geometry quite easily. Figure 3a shows a mesh used in the present study (with $L/h = 15$), which was designed automatically using a procedure that minimizes the finite element error for elastic problems [10]; this leads to very small elements at the top and bottom of the PSB.

Several type B PSB aspect ratios between **3** and 100 have been considered, with a different mesh for each value. In each case, an alternating uniaxial remote stress was applied until stabilization was reached (which required about 10 cycles); the largest plastic slip was always obtained at the free surface (Figure 4a) for $L/h = 15$, for instance), and the average and largest surface effect ratios were computed. They were defined by considering PSBs with the same aspect ratios in both the volume and the surface problems, because this is the most harmful situation for a fixed grain size: for a grain in the hulk, the length of the largest PSB is about the grain diameter, and this may apply to an almost equiaxed surface grain. As shown in Figure 4b, r_{ave} and r_{max} are quite constant, with $r_{ave} \approx 1.9$ and $r_{max} \approx 2.5$, for aspect ratios in the 10–100 range. Comparing bands of the same length and thickness gives a surface effect ratio r_{ave} about 1.9 in the 10–100 range of aspect ratios. It should finally be noted that these weak variations of the surface effect ratios imply that the surface plastic slips are roughly proportional to L/h, like in the volume cases.

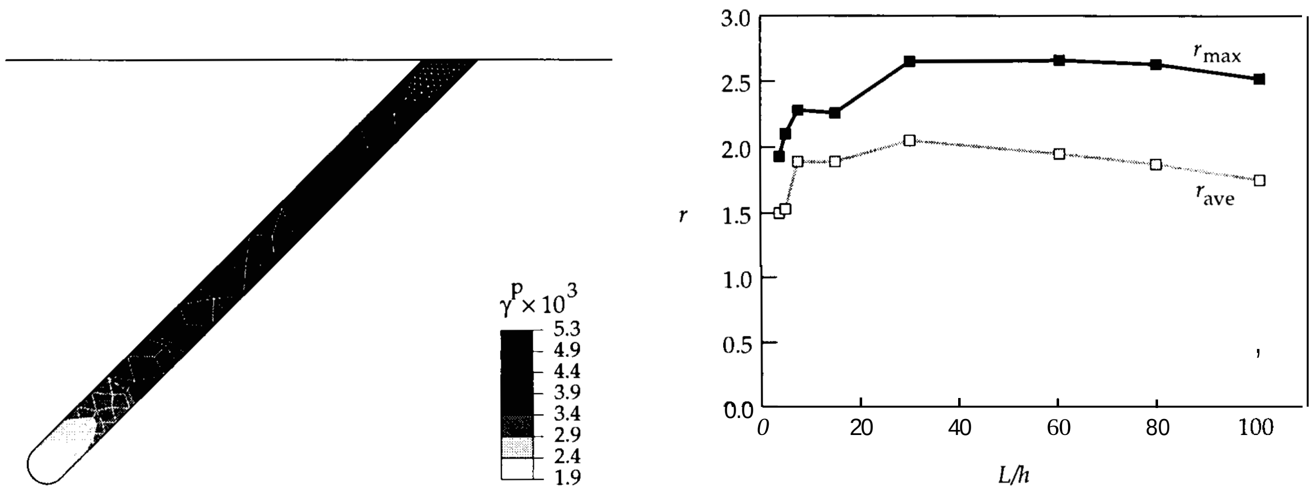

(a) (b)

Figure 4 (a): Contours of the γ^p amplitude in a surface PSB of type B, for an alternating uniaxial remote stress. $E = 200$ GPa, $\nu = \mathbf{0.3}$, $b = 1000$, $\tau_0 = \mathbf{30}$ MPa, $\tau_\infty = 49$ MPa, C, $= 0$, C, $= 125$ MPa. (b): Variations of the surface effect ratios r_{max} and r_{ave} with the aspect ratio L/h of a type B PSB. Same parameters.

APPLICATION TO CRACK NUCLEATION

The nucleation of cracks has been explained by different mechanisms. One of them appears to be important in polycrystals [1]. After saturation, the behavior in the PSB is accommodated at the mesoscale (scale of the order of 1μ) with the cyclic plastic slips computed above. For the sake of simplicity, the mesoscopic slip $\Delta\gamma^p$ is supposed to be homogeneous with the average value computed above. It is well-known nevertheless that there are plastic irreversibilities at a smaller (microscopic) scale (Figure 5) [1].At each cycle, residual microscopic positive or negative slips $\delta\gamma^p(\boldsymbol{P},N)$ appear at the microscopic scale. These increments depend on the point $\boldsymbol{P}$ in the PSB and on the cycle N. They are cumulated along time, enhancing the stored elastic energy because of incompatibilities between the PSB and the matrix around. They induce an increasingly pronounced relief at the free surface too (Figures 1 and 5). The irreversibility factor f_{irr} is classically defined by:

$$f_{irr} = \frac{< |\delta\gamma^p(.,N)| >_{PSB}}{\Delta\gamma^p} \tag{6}$$

where $\Delta\gamma^p$ is the mesoscopic plastic slip range as above, $< |\delta\gamma^p(.,N)| >_{PSB}$ is the average on the PSB of the magnitudes of the microscopic plastic slip increments [1]. Several physical phenomena explain this microscopic irreversibility: different paths for the forward and reverse glide of dislocations during a cycle, dislocations vanishing through the free surface, environmental interactions like adsorption or oxidation... [12].

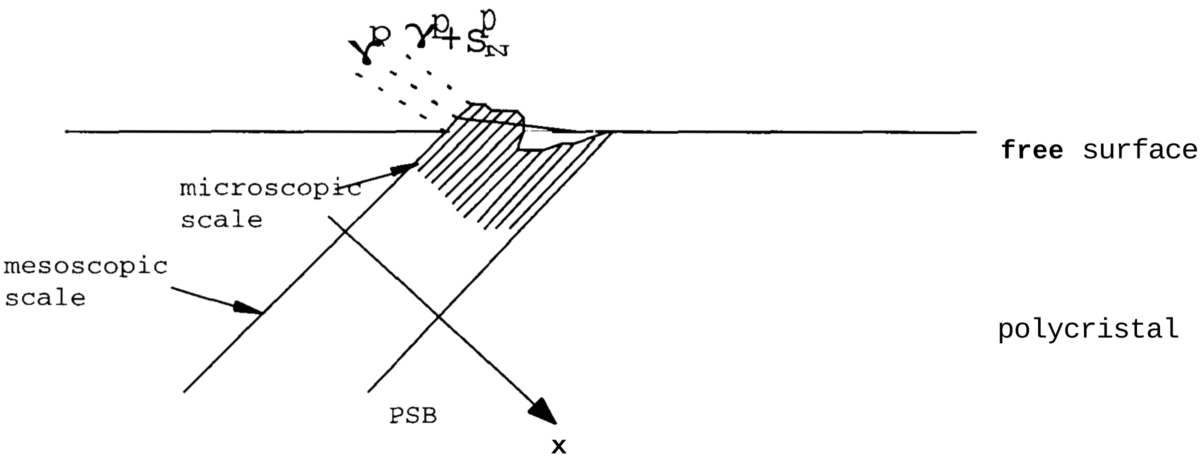

Figure 5*:* Mesoscopic and microscopic plastic slips in a surface PSB. The microscopic slips are partially irreversible.

Following a bulk model of Mura and co-workers, we model this mechanism in the framework of continuous mechanics, using a statistical approach [6]. The increments $\delta\gamma^p(\boldsymbol{P}, N)$ are supposed to be of the same random nature and independent in terms of probability. For the sake of simplicity, $\delta\gamma^p$ can take any value in between $-\delta\gamma^p_{max}$ and $+\delta\gamma^p_{max}$ with the same probability. The statistical distribution is defined by: $f(\delta\gamma^p) = \frac{1}{2\delta\gamma^p_{max}}$ if $-\delta\gamma^p_{max} < \delta\gamma^p < \delta\gamma^p_{max}$ and $f(\delta\gamma^p) = 0$ otherwise. Then the statistical mean and the variance are equal to $\overline{\delta\gamma^p} = 0$ and $\overline{(\delta\gamma^p)^2} = (\delta\gamma^p_{max})^2/3$ where $\overline{(.)}$ denotes the statistical mean. In addition: $\overline{|\delta\gamma^p|} = \frac{\delta\gamma^p_{max}}{2}$. Because of assumed ergodicity, the space averages and the statistical means are equal, then $f_{irr} = \frac{\overline{|\delta\gamma^p|}}{\Delta\gamma^p}$ and the only statistical parameter $\delta\gamma^p_{max}$ can be defined by the irreversibility factor f_{irr} and by our computed value of $\Delta\gamma^p$: $\delta\gamma^p_{max} = 2f_{irr}\Delta\gamma^p$. It follows: $\overline{(\delta\gamma^p)^2} = \frac{4}{3}(f_{irr})^2(\Delta\gamma^p)^2$. The increments are cumulated along the cycles, inducing a slip $s^p_N(\boldsymbol{P}) = \sum_{i=1}^{N}\delta\gamma^p(\boldsymbol{P}, i)$. The central limit theorem states that the distribution of the microscopic cumulated slip $s^p_N(\boldsymbol{P})$ approaches a Gaussian distribution with a mean equal to 0 and a variance equal to $N\overline{(\delta\gamma^p)^2} = \frac{4}{3}(f_{irr})^2(\Delta\gamma^p)^2$.

In this model, cracks are supposed to appear suddenly along the bulk or surface PSBs leading to an energy criterion:

$$\overline{\Delta W(N_n)} = 4LW_s \tag{7}$$

with $\Delta W(N)$ the variation of the stored energy in the solid at the $N_n\hat{\text{t}}\text{h}$ cycle due to the crack nucleation (number of cycles after saturation). The stored energy is the sum of the elastic stored energy and of the potential energy due to the remote macroscopic stress C applied on the boundaries. *W,* is the surface energy of the material.
For small remote stresses and $L >> h$, lengthy computations lead to [13,14]:

$$N_n \approx \frac{24(1-\nu)}{\pi\mu}\frac{W_sL}{h^2}\frac{1}{(f_{irr})^2(\Delta\gamma^p)^2} \approx C\frac{24\mu}{\pi(1-\nu)}\frac{W_s}{L}\frac{1}{(f_{irr})^2(\Sigma_a - 2\tau_\infty)^2} \tag{8}$$

with C = 1 for a bulk PSB and C = $\frac{1}{r_{ave}}$ for a surface PSB. These equations extend the formula proposed by Mura and co-workers [6,13] to the surface case. Finally, the nucleation number ratio can be approximately computed using the $\frac{\Delta\gamma^p_{vol}}{\Delta\gamma^p_{surf}}$, $\frac{f^{vol}_{irr}}{f^{surf}_{irr}}$ and $\frac{W^{surf}_s}{W^{vol}_s}$ ratios:

$$\frac{N^{surf}_n}{N^{vol}_n} \approx \frac{\Delta\gamma^p_{vol}}{\Delta\gamma^p_{surf}}\left(\frac{f^{vol}_{irr}}{f^{surf}_{irr}}\right)^2\frac{W^{surf}_s}{W^{vol}_s} \tag{9}$$

DISCUSSION

Since the stress level is low in high-cycle fatigue, single slip has been assumed throughout this study, and this allows extending the proposed analyses to any material deforming by crystallographic slip, whatever its structure: only the largest affordable remote stress level is modified, which is limited by the activation of a second system. Moreover, the assumption that a stabilized behavior is reached implies that the computed surface effect ratios r_{ave} and $r_{\max}$ depend essentially on τ_∞/μ and Σ_a/μ for an alterning load, a priori. Indeed, the saturation critical resolved shear stress, the remote stress and the elastic shear modulus are the only reference stresses left in the computations, and the Poisson's ratio is without significant influence on the ratios. Varying the τ_∞ and C, values, with a constant p value, the same r_{ave} and $r_{\max}$ estimation have been obtained. This allows a further extension of the results to usual polycrystals.

Our evaluations of plastic slip in surface PSBs agree qualitatively with experimental results of Mughrabi and Wang [7] on surface cyclic microplasticity of Cu polycrystals. These authors observed that surface PSBs are deformed more than in the bulk, and they deduced from indirect measures that this concerns particularly type B surface PSBs, which agrees with our conclusions. Moreover, Mughrabi [2] reports experimental slip magnitudes of at least $12 10^{-3}$ in PSBs in ferrite single crystals with 30 wt. ppm carbon. Since smaller slips are expected for more constrained PSBs, this figure is consistent with the $8.6\,10^{-3}$ and $4.2\,10^{-3}$ values we compute for surface and volume PSBs, respectively (choosing $\frac{L}{h} = 15$).

As it is difficult to measure or to compute the irreversibility factors, the ratio $\frac{f_{irr}^{vol}}{f_{irr}^{surf}}$ is considered to be equal to 1, but is probably smaller than 1 (because of free surface and environmental effects). Figure 6 shows computed Woehler's curves for a copper polycristal. The first curve takes into account the enhanced mesoscopic plasticity and the lowering of the surface energy W_s because of environmental effects. The second considers only the mesoscopic plasticity effect and the third represents the bulk case. Taking into account the two effects gives a number of cycles to nucleation (after saturation) about six times smaller than in the bulk, which agrees with the experimental results of Thomson et al. [15] and Basinski et al. [16]. These authors have shown that elimination of the surface roughness by electropolishing the specimen surface enhances greatly the fatigue life. If the ratio $\frac{f_{irr}^{vol}}{f_{irr}^{surf}}$ could be evaluated, our predicted nucleation life ratio would have been smaller.

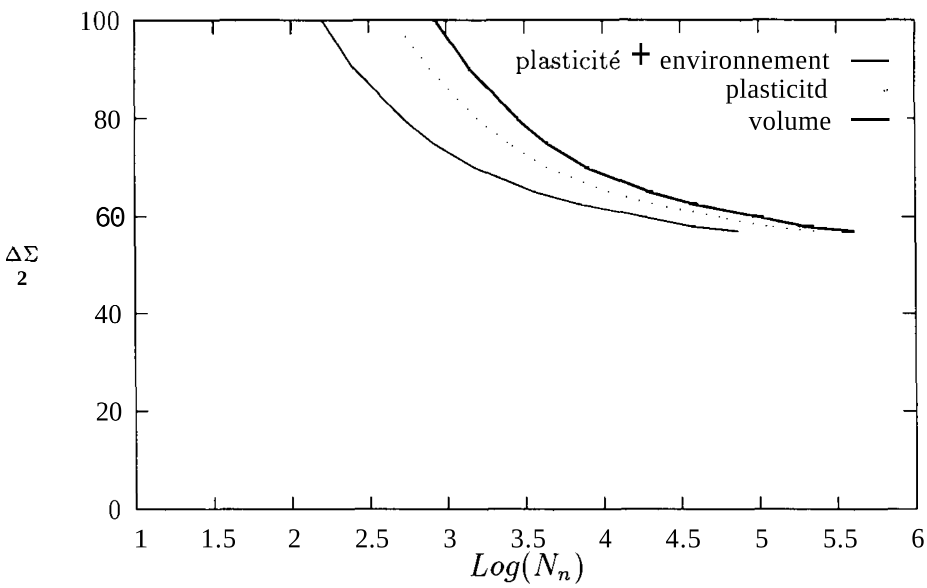

Figure 6: Woehler's curves at nucleation for a copper polycristal using (S). $E = 112\,\text{GPa}$, $\nu = 0.35$, $\tau_\infty = 28$ MPa [2], $L = 50\mu$, $f_{irr}^{vol} = f_{irr}^{surf} = 0.1$ [1],$W_s^{vol} = 1.65$ N/m, $W_s^{surf} = 0.55$ N/m [13] and

$C_s = 0$.

Some physical characteristics have been neglected in this work. Taking into account the elastic crystalline anisotropy, several PSBs appearing in the same grain, or the extrusions/intrusions forming at the beginning of the fatigue life inducing stress concentrations at the free surface (Figure 1) [1,17] would improve this first approach of the surface effects in polycyclic fatigue of metals.

CONCLUSION

Using analytical and finite element computations, the cyclic range of mesoplastic slip in type B PSBs during uniaxial fatigue has been evaluated. In practical applications, the surface plastic slips are obtained by first computing analytically the result for a PSB in an infinite matrix, and multiplying by the corresponding $r_{\mathbf{ave}}$ or $r_{\mathbf{max}}$ value given in this work. The factors ares $r_{\mathbf{ave}} \approx 1.9$ and $r_{\mathbf{max}} \approx 2.5$ for a type B orientation. An energy criterion has been applied to the nucleation of microcracks along a surface PSB. This model considers the plastic slips irreversibilities at the microscopic scale and takes into account partially the free surface and the environmental effects. The nucleation in the bulk seems to be significantly delayed because of the two effects. The predicted increase of plastic slip and decrease of number of cycles to nucleation agree with several experimental results concerning cyclic surface plasticity and damage. Our computations may thus help to predict crack nucleation.

Acknowledgments

This project was supported by Ledepp, USINOR Recherche et Développement. Professor J. Lemaitre is acknowledged for his interest in this research.

References

[1] Mughrabi H., Wang R., Differt K. and Essmann U. (1983). In: *Fatigue Mechanisms: Advances in Quantitative Measurement of Physical Damage ASTM STP 811*, pp. 5-45, Lankford J., Davidson D. L., Morris W. L., and Wei R. P. (Eds). American Society for Testing and Materials.

[2] Mughrabi H.(1979). In: *Strength of Metals and Alloys*, pp. 1615-1638, Haasen P., Gerold V. and Kostorz G. (Eds). Pergamon.

[3] Man J., Obrtlik K., Lopour F., Blochwitz C., Polák J. (1999). In: *Proceedings of the seventh International Fatigue Congress*, pp. 157-162. Higher Education Press.

[4] Hempel M. (1956). In: *ASME and IMechE International Conference on the Fatigue of Metals*, pp. 543-547. Institution of Mechanical Engineers, London.

[5] Sauzay M. and Gilormini P. (2000). *Fatigue Fract. Engng Mater. Struct.*, in the press.

[6] Kato M., Onaka S., Mori T., Mura T. (1984). *Scripta Metall.* **18,** 1323.

[7] Mughrabi H. and Wang R. (1988). In: *Basic Mechanisms in Fatigue of Metals*, pp. 1-13, Lukas P. and Polak J. (Eds). Elsevier.

[8] Eshelby J. D. (1957). *Proc. Roy. Soc. Lon. A* **241,** 376.

[9] Mura T. (1982). *Micromechanics of Defects in Solids.* Martinus Nijhoff Publishers.

[10] Coorevits P., Ladèveze P. and Pelle J.P. (1995). *Comp. Meth. Appl. Mech. Engng* **121,** 91

[11] Doquet V. (1997). *Fatigue Fract. Engng Mater. Struct.* **20,** 227.

[12] Suresh S. (1991). *Fatigue of materials.* Cambridge University Press.

[13] Venkataraman G., Chung Y-W., Nakasone Y. and Mura T. (1990). *Acta Metall. Mates..* **38 1**, 31.

[14] Sauzay M. (2000). PhD Thesis, Université Paris VI, France.

[15] Thomson N., Wadsworth N. J., Louat N. (1956). *Phil. Mag* **1,** 113.

[16] Basinski Z. S., Pascual R., Basinski S. J. (1983). *Acta. Metall. Mater.* **31,** 591.

[17] Brown L. M. and Ogin S. L. (1985). In: *Fundamentals of deformation and fracture – IUTAM Eshelby Memorial Symposium*, pp. 501-528, Bilby B. **A.,** Miller K. J. and Willis J. R. (Eds). Cambridge University Press.